Revisiting the Helium Isotope-Shift Puzzle with Improved Uncertainties from Nuclear Structure Corrections

Revisiting the Helium Isotope-Shift Puzzle with Improved Uncertainties from Nuclear Structure Corrections

Simone Salvatore Li Muli,[1,2,*] Thomas R. Richardson,[1,†] and Sonia Bacca[1,3,‡]
[1]Institut für Kernphysik and PRISMA$_+$ Cluster of Excellence, Johannes Gutenberg-Universität, 55128 Mainz, Germany
[2]Department of Physics, Chalmers University of Technology, SE-412 96 Göteborg, Sweden
[3]Helmholtz-Institut Mainz, Johannes Gutenberg-Universität Mainz, D-55099 Mainz, Germany

(Received 30 January 2024; revised 11 July 2024; accepted 16 December 2024; published 23 January 2025)

Measurements of the difference between the squared charge radii of the helion (^{3}He nucleus) and the α particle (^{4}He nucleus) have been characterized by longstanding tensions recently spotlighted in the 3.6σ discrepancy of the extractions from ordinary atoms versus those from muonic atoms [Karsten Schuhmann *et al.*, arXiv:2305.11679]. Here, we present a novel analysis of uncertainties in nuclear structure corrections that must be supplied by theory to enable the extraction of the difference in radii from spectroscopic experiments. We use modern Bayesian inference techniques to quantify uncertainties stemming from the truncation of the chiral effective field theory expansion of the nuclear force for both muonic and ordinary atoms. With the new nuclear structure input, the helium isotope-shift puzzle cannot be explained, rather, it is reinforced to a 4σ discrepancy.

DOI: 10.1103/PhysRevLett.134.032502

Introduction—Historically, atomic physics has played a central role in shaping modern physics. Explaining the gross features of the hydrogen-atom spectrum led to the development of quantum mechanics [1,2], studying its fine-structure details inspired relativistic quantum mechanics [3], and the discovery of the Lamb shift [4] gave rise to the theory of quantum electrodynamics (QED) [5–7]. While the hydrogen atom is still a protagonist [8–10], other simple atomic systems, such as hydrogenlike ions [11] or two-electron atoms [12,13], have entered the scenery of high-precision laser spectroscopy. Today, atomic physics is experiencing an exciting time, when not only fundamental constants—such as the Rydberg constant [14]—are determined with better than ever precision, but the comparison of results from multiple experiments on a variety of simple and calculable systems allows for fruitful intersections with particle, hadronic, and nuclear physics [15,16]. In fact, high-precision laser spectroscopy can be used as a rigorous test of the standard model and has the potential to constrain sources of beyond the standard model physics. Furthermore, muonic atom spectroscopy allows for precise determinations of the size of the nucleus [17–21] and nuclear polarizability effect [19] because the mass of the muon, approximately 200 times that of the electron, makes the muon very sensitive to nuclear structure.

Recently, the difference between the squared charge radius of the helion (^{3}He nucleus) and the α particle (^{4}He nucleus) defined as $\delta r^2 = r^2_{\mathrm{ch}}(^3\mathrm{He}) - r^2_{\mathrm{ch}}(^4\mathrm{He})$ has attracted significant attention [21–28]. This difference can be extracted from the isotope shifts of the $2^3S \to 2^1S$ transition [22–24], the $2^3S \to 2^3P$ transition [25–27], and the $2^1S \to 2^1D$ transition [28], but the obtained values vary quite substantially; see Fig. 5 in Ref. [21] for a summary. In particular, results from the same group in Refs. [22–24] are in disagreement; however, a reanalysis confirmed that the differences are understood and that the most recent experiment [24] supersedes the older two [22,23]. The final value inferred from Ref. [24] is $\delta r^2|_e = 1.0757(15)$ fm^2.

The difference in the charge radii obtained from the isotope shift in ordinary atoms can be compared to the results obtained from muonic atoms. In the latter, the absolute values of the individual radii can be extracted from Lamb-shift measurements. The sizes of ^{3}He [20] and ^{4}He [21] were recently measured by the CREMA Collaboration resulting in $\delta r^2|_\mu = 1.0636(6)^{\mathrm{expt}}(30)^{\mathrm{theo}}$ fm^2 [21]. Comparing this value to the most recent measurement based on the isotope shifts in ordinary atoms, in particular, the measurement of Ref. [24], reveals a 3.6σ discrepancy. The error bars in radii extractions from muonic atom experiments are largely dominated by uncertainties coming from theoretical calculations of nuclear structure corrections. In this work, we use modern Bayesian inference to solidly quantify uncertainties in such calculations.

*Contact author: simone.limuli@chalmers.se
†Contact author: richardt@uni-mainz.de
‡Contact author: s.bacca@uni-mainz.de

Nuclear structure corrections—The observed energy spectrum of an atom differs from that obtained via the solution of the Schrödinger or Dirac equation in a static Coulomb potential because of QED, nuclear recoil, and nuclear structure effects. The difference of the two energy levels in an atom containing a ^{A}He nucleus is parametrized as

$$\Delta E = \delta_{\rm QED} + \mathcal{C} r_{\rm ch}^2 + \delta_{\rm NS}. \tag{1}$$

In Eq. (1), $\delta_{\rm QED}$ comprises purely QED and nuclear recoil effects, and the second term is a nuclear finite-size effect where $\mathcal{C}$ is a known constant for each of the transitions considered. The last term $\delta_{\rm NS}$ contains nuclear structure corrections that begin with the exchange of two photons. At the level of two-photon exchange, these corrections enter through the nuclear matrix elements of the forward virtual Compton tensor [29] and constitute the dominant source of uncertainty in the extraction of $r_{\rm ch}$ from muonic atom spectroscopy [30–32].

The $\delta_{\rm NS}$ is expanded as

$$\delta_{\rm NS} = \delta_{\rm TPE} + \delta_{\rm 3PE} + \delta_{\rm EVP} + \delta_{\rm MSEVP} + \cdots, \tag{2}$$

where the terms include two-photon exchange $\delta_{\rm TPE}$, three-photon exchange $\delta_{\rm 3PE}$, electron vacuum polarization $\delta_{\rm EVP}$, and muon self-energy and vacuum polarization $\delta_{\rm MSEVP}$ corrections. For muonic atoms, the last three terms have been recently discussed in Ref. [30] (note that in [30], the last two terms are labeled sightly differently, with eVP and μSE, respectively). In this work, we focus on the two-photon-exchange term, which can be written as [33,34]

$$\begin{aligned}\delta_{\rm TPE} &= \delta^A_{\rm TPE} + \delta^N_{\rm TPE} \\ &= \delta^A_{\rm Zem} + \delta^A_{\rm pol} + \delta^N_{\rm Zem} + \delta^N_{\rm pol},\end{aligned} \tag{3}$$

where $\delta^A_{\rm Zem}$ ($\delta^N_{\rm Zem}$) denotes nuclear (single-nucleon) elastic or Zemach contributions, and $\delta^A_{\rm pol}$ ($\delta^N_{\rm pol}$) denotes nuclear (single-nucleon) inelastic or polarizability contributions. In both muonic and ordinary atoms, the Zemach contribution will be canceled by a piece of the polarizability correction [29,35,36]. In the remainder of this work, we denote the two-photon-exchange contributions in muonic (ordinary) atoms by $\delta^A_{{\rm TPE},\mu}$ ($\delta^A_{{\rm TPE},e}$).

In muonic atoms, the nuclear excitation energy is generally much smaller than the muon mass. In the so-called η-expansion formulation [29,33,34,37,38], where $\eta \simeq \sqrt{m_r/m_p}$ and m_r, m_p are the reduced mass of the muon-nucleus system and the proton mass, respectively, the two-photon-exchange correction can be decomposed in multipoles leading to a dipole contribution and higher-order terms. Explicit expressions for these terms up to the second power in the η expansion, as well as the Zemach term may be found in Ref. [34] and are therefore not repeated here. Using Bayesian inference, in Ref. [38] the value of η was found to be 0.15 (0.35) for muonic ^{4}He (^{3}He), respectively.

For electronic atoms, the opposite scenario is realized where the nuclear excitation energy ω_N is generally much larger than the electron mass m. In this case, the leading contribution from nuclear structure effects is [39,40]

$$\delta^A_{{\rm TPE},e} = -\frac{2}{3} m (Z\alpha)^2 \phi^2_{nS} \tilde{\alpha}_{{\rm pol},e}, \tag{4}$$

where ϕ_{nS} is the electronic wave function at the origin, Z is the proton number, α is the fine structure constant, and

$$\tilde{\alpha}_{{\rm pol},e} = \sum_{N\neq 0} |\langle N|\mathbf{D}|0\rangle|^2 \left[\frac{19}{6\omega_N} + \frac{5\ln(2\omega_N/m)}{\omega_N}\right], \tag{5}$$

where $\mathbf{D}$ is the electric-dipole operator. We neglect higher-order terms as they are found to be small (1% in the deuterium $1S$-$2S$ transition [39]), but we will later include an uncertainty to account for this assumption.

We evaluate $\delta^A_{{\rm TPE},\mu}$ and $\tilde{\alpha}_{{\rm pol},e}$ by solving the few-nucleon Schrödinger equation to obtain $|0\rangle$ and $|N\rangle$ via the effective interaction hyperspherical harmonics (EIHH) method, which is accurate at the subpercent level for three- and four-body problems [41–44]. We use nuclear forces derived from chiral effective field theory (χEFT) [45–48]. There are many families of χEFT interactions available in the literature. Given that the EIHH method can presently use general two-nucleon forces, but only local three-nucleon forces, following Refs. [44,49], for the first three orders we use the local formulation of Refs. [50–52], with three-body forces entering at next-to-next-to-leading order (N2LO), and adopt the cutoffs $r_0 = 1.0$ fm and $r_0 = 1.2$ fm (see Supplemental Material [53]). For the last order, we take the nonlocal two-body force from Ref. [54] at next-to-next-to-next-to-leading order (N3LO) supplemented by the local N2LO three-body forces from Ref. [55]; this combination has been used before in Refs. [33,34,56]. We point out that with these choices we are exploring quite different interaction models. On the one hand, we use both local [50–52] and nonlocal [54] two-body forces with different cutoffs. On the other hand, we adopt two strategies for the fit of the low-energy constants c_D and c_E entering the three-body force at N2LO: For [50–52], they are constrained to reproduce the ^{4}He binding energy and the $n-\alpha$ P-wave phase shifts, while for [55], c_E is kept natural and c_D is fit on the ^{3}H binding energy. While other choices are possible (see, e.g., [57]), we believe that this combination of forces captures most of the potential model dependences.

Bayesian uncertainty quantification—The truncation error of the χEFT expansion is quantified by calculating nuclear structure corrections at different orders. Bayesian inference can be used to analyze the convergence pattern of any observable with respect to a reference $\mathcal{O}^{\rm ref}$,

$$\mathcal{O} = \mathcal{O}_{\rm ref} \sum_{n=0}^{\infty} c_n Q^n, \tag{6}$$

where the expansion parameter Q is related to the natural energy scale of the process and Λ, the breakdown scale of χEFT, as $Q = \max\{m_\pi, p\}/\Lambda$, with m_π being the pion mass and p the average involved low-energy momentum. Here, we choose $\Lambda \sim 500$ MeV, which is consistent with Refs. [50–52], $Q = m_\pi/\Lambda$ for ^{3}He, and $Q = p/\Lambda$ for ^{4}He, where we take $p \sim 180$ MeV as the average nucleon momentum in the nucleus [58]. The expansion coefficients c_n are obtained by calculating the observable at each fixed chiral order. For $\mathcal{O}_{\rm ref}$, we take results obtained with the phenomenological AV18 + UIX potential [we obtain similar results if we instead use the leading-order (LO) chiral result as $\mathcal{O}^{\rm ref}$].

We assume that all of the expansion coefficients c_n are of natural size set by the same scale parameter $\bar{c}$. These assumptions are encoded in the use of Jeffrey's prior [59] for $\bar{c}$ and Gaussian priors for each c_n. Explicitly, the prior probability density functions are

$$\begin{aligned} {\rm Prob}(\bar{c}) &= \frac{1}{\ln(\bar{c}_>/\bar{c}_<)\bar{c}}\theta(\bar{c}-\bar{c}_<)\theta(\bar{c}_>-\bar{c}), \\ {\rm Prob}(c_n|\bar{c}) &= \frac{1}{\sqrt{2\pi}\bar{c}}\exp\left[-\frac{c_n^2}{2\bar{c}^2}\right], \end{aligned} \tag{7}$$

where $\bar{c}_> = 10^3$, $\bar{c}_< = 10^{-3}$, and the two theta functions constrain $\bar{c}_< < \bar{c} < \bar{c}_>$, so that the probability distribution ${\rm Prob}(\bar{c})$ is normalizable. With these prior choices, the truncation error follows a Gaussian $\mathcal{G}$ distribution, ${\rm Prob}(\mathcal{O}_{\rm ref}\Delta_k|\bar{c}, Q) = \mathcal{G}(0, \sigma^2)$, where k is the order of the χEFT expansion, and the standard deviation is $\sigma^2 = \mathcal{O}_{\rm ref}^2\bar{c}^2Q^{2k+2}/(1-Q^2)$ [60]. By marginalizing over $\bar{c}$ and by applying Bayes theorem, the posterior probability distribution for the truncation error becomes [38,61]

$${\rm Prob}(\Delta_k|\mathbf{c}, Q) = \frac{\int d\bar{c}\,{\rm Prob}(\Delta_k|\bar{c}, Q)\left[\prod_{n=0}^{k}{\rm Prob}(c_n|\bar{c})\right]{\rm Prob}(\bar{c})}{\int d\bar{c}\left[\prod_{n=0}^{k}{\rm Prob}(c_n|\bar{c})\right]{\rm Prob}(\bar{c})}, \tag{8}$$

where the coefficients $\mathbf{c} = \{c_0, \ldots, c_k\}$ are known from our order-by-order calculation of the observable in χEFT.

Results—In Fig. 1, we show probability density functions (PDFs) obtained via a Bayesian analysis for values of $\delta^A_{{\rm TPE},\mu}$ representing our best estimates for the truncation uncertainties of the χEFT expansion. The first row shows the uncertainty from truncating the χEFT expansion at LO, the second row at NLO, the third row at N2LO, and the last row at N3LO. The dark shaded areas are 68% confidence intervals while the light shaded areas are 95% confidence intervals. The vertical black lines are the predictions for $\delta^A_{{\rm TPE},\mu}$ obtained with the AV18 + UIX interaction. We note that our LO results are very different from the other orders. This is due to the fact that the expansion coefficient c_0 is much smaller than the other coefficients; see Supplemental Material [53].

In Refs. [33,34], the uncertainty quantification was performed by comparing the prediction of the N3LO chiral interaction to that of the phenomenological AV18 + UIX. Here, the Bayesian analysis leads to an improved error estimate established on solid statistical ground. The most precise values are obtained at N3LO, where we find $\delta^A_{{\rm TPE},\mu} = -14.868(364)$ meV in $\mu^3{\rm He}^+$ and $\delta^A_{{\rm TPE},\mu} = -8.751(322)$ meV in $\mu^4{\rm He}^+$. The uncertainties are obtained as quadrature sums of the Bayesians χEFT expansion error and the remaining sources of uncertainty; see Supplemental Material [53]. Our results can be compared to the previous calculations, $\delta^A_{{\rm TPE},\mu} = -14.72(31)$ meV in $\mu^3{\rm He}^+$ [34,56] and $\delta^A_{{\rm TPE},\mu} = -8.49(39)$ meV in $\mu^4{\rm He}^+$ [33,34], from which it is evident that our estimation based on Bayesian inference increases the uncertainty in $\delta^A_{{\rm TPE},\mu}$ of

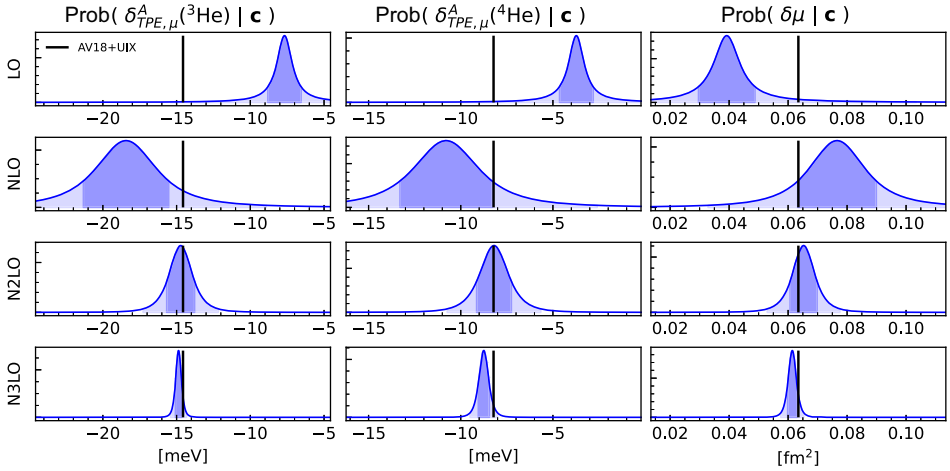

FIG. 1. Bayesian analysis of the χEFT expansion in muonic helium (vertical lines are the AV18 + UIX results [34]).

TABLE I. Nuclear structure effects in muonic helium at N3LO and extracted charge radii.

	$\delta^A_{\mathrm{TPE},\mu}$ (meV)	$\delta_{\mathrm{NS},\mu}$ (meV)	r_{ch} (fm)
^{3}He	−14.868(364)	−15.644(427)	1.9704(11)
^{4}He	−8.751(322)	−9.541(368)	1.6793(10)

$\mu^3\mathrm{He}^+$ by 17%, but reduces the uncertainty in $\mu^4\mathrm{He}^+$ by 17%. The increased uncertainty in $\mu^3\mathrm{He}^+$ is mostly due to an update of the uncertainty associated with the η expansion [38]. These results for $\delta^A_{\mathrm{TPE},\mu}$ may be combined with remaining terms in Eq. (2) to produce $\delta_{\mathrm{NS},\mu}$. The charge radii of ^{3}He and ^{4}He can be found by solving Eq. (1) for r_{ch} using the measured Lamb shift [20,21]. A summary of these results can be found in Table I. For ^{4}He, this constitutes the most precise extraction of the nuclear charge radius to date.

In Fig. 2, we show the PDFs for $\tilde{\alpha}_{\mathrm{pol}}$ representing the evolution of this observable, and of the associated uncertainty, as we increase the order of the χEFT expansion of the nuclear Hamiltonian. The expansion shows identical features to those of Fig. 1. At N3LO, we obtain $\tilde{\alpha}_{\mathrm{pol}} = 3.514(68)$ and $1.909(96)$ fm^3 for ^{3}He and ^{4}He, respectively. Within uncertainties, our results are compatible with the values of 3.56(36) and 2.07(20) fm^3 estimated in Ref. [40] for ^{3}He and ^{4}He, respectively.

Revisiting the helium isotope shift—Starting from our new calculations of nuclear structure effects in atomic spectra, we update the extraction of δr^2 [21,24], considering the Lamb-shift $2S \to 2P$ transition for muonic atoms and the $2^3S \to 2^1S$ isotope shift for ordinary atoms. First, we invert Eq. (1) to obtain the squared charge radius of the individual nuclei, and then we take the difference between ^{4}He and ^{3}He,

$$\delta r^2 = \left[\frac{\Delta E(^3\mathrm{He})}{\mathcal{C}(^3\mathrm{He})} - \frac{\Delta E(^4\mathrm{He})}{\mathcal{C}(^4\mathrm{He})}\right] + \left[\frac{\delta_{\mathrm{QED}}(^4\mathrm{He})}{\mathcal{C}(^4\mathrm{He})} - \frac{\delta_{\mathrm{QED}}(^3\mathrm{He})}{\mathcal{C}(^3\mathrm{He})}\right] + \left[\frac{\delta_{\mathrm{NS}}(^4\mathrm{He})}{\mathcal{C}(^4\mathrm{He})} - \frac{\delta_{\mathrm{NS}}(^3\mathrm{He})}{\mathcal{C}(^3\mathrm{He})}\right]. \tag{9}$$

The last term in Eq. (9) contains the difference of δ_{NS} between ^{4}He and ^{3}He. For δ^N_{TPE} in Eq. (3) and δ_{3PE}, δ_{EVP}, and δ_{MSEVP} in Eq. (2), we use the values from Ref. [30] and analyze the part which we newly calculated, namely,

$$\delta\mu = \left[\frac{\delta^A_{\mathrm{TPE},\mu}(^4\mathrm{He})}{\mathcal{C}(^4\mathrm{He})} - \frac{\delta^A_{\mathrm{TPE},\mu}(^3\mathrm{He})}{\mathcal{C}(^3\mathrm{He})}\right], \tag{10}$$

$$\delta e = \left[\tilde{\alpha}_{\mathrm{pol},e}(^4\mathrm{He}) - \tilde{\alpha}_{\mathrm{pol},e}(^3\mathrm{He})\right]\frac{1}{\mathcal{C}}, \tag{11}$$

for muonic atoms and ordinary atoms, respectively (note that the constant $\mathcal{C}$ is the same for ^{3,4}He [62] for the isotope shift of this transition in ordinary atoms). We perform a Bayesian analysis of this difference, which will naturally take correlations between ^{3}He and ^{4}He into account.

The results of the statistical analysis of $\delta\mu$ and δe for each chiral order are shown in Figs. 1 and 2, respectively. At N3LO, we obtain $\delta\mu = 0.0614(16)(20)$ fm^2, where the first uncertainty comes from the Bayesian analysis of the χEFT expansion, while the second includes all the rest, explained in Supplemental Material [53]. To estimate the latter, from our Bayesian analysis we extracted the correlation coefficient between the two terms in Eq. (10), amounting to 0.84, and used it to propagate the uncertainties to $\delta\mu$. Compared to $\delta\mu = 0.0624(42)$ fm^2 obtained in Ref. [34], the new result constitutes a significant reduction of the uncertainties due to the inclusion of correlations between ^{3}He and ^{4}He. Using values for ΔE, δ_{QED}, and $\mathcal{C}$ reported in Table III of Supplemental Material [53], and

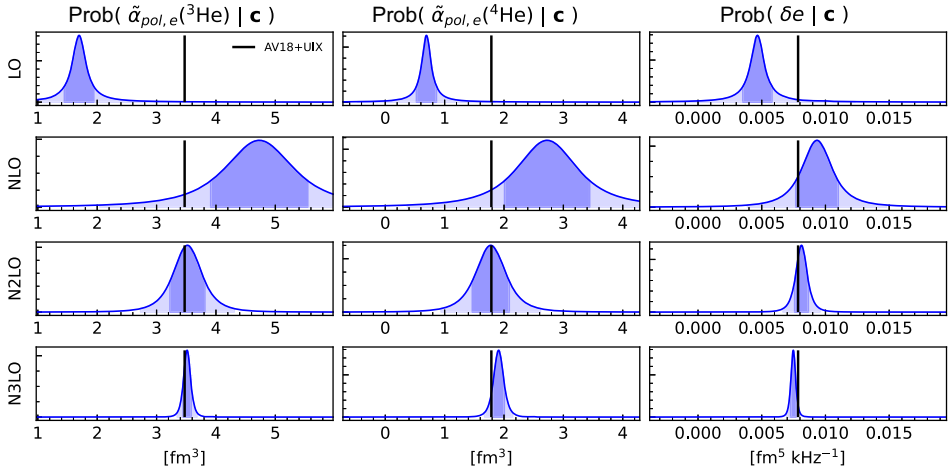

FIG. 2. Same as Fig. 1 for $\tilde{\alpha}_{\mathrm{pol}}$ in ordinary helium atoms.

assuming that $\delta_{\rm 3PE}$, $\delta_{\rm EVP}$, and $\delta_{\rm MSEVP}$ in ^{3}He and ^{4}He are correlated in the same way as $\delta^A_{\rm TPE}$, we obtain

$$\delta r^2|_\mu = 1.0626(29)\ \text{fm}^2 \tag{12}$$

for muonic atoms. This improves the uncertainty of the previous determination, $\delta r^2|_\mu = 1.0636(31)$ fm^2 [21] by about 6%.

For ordinary atoms, we obtain $\delta e = 0.00748(21)\ \text{fm}^5\,\text{kHz}^{-1}$ at N3LO, which can be compared with $\delta e = 0.0069(19)\ \text{fm}^5\,\text{kHz}^{-1}$ from Ref. [40]. The uncertainty in Ref. [40] is attributed to higher-order terms in Eqs. (4) and (5) that were neglected. This uncertainty was estimated to be of the order of 10% [40]; however, there was no attempt to estimate the uncertainties associated with the model dependence of the dipole polarizability. In this work, we rigorously quantify the latter, while we assume 10% uncertainty to account for the former, resulting in $\delta e = 0.00748(96)\ \text{fm}^5\,\text{kHz}^{-1}$. Using values for ΔE, $\delta_{\rm QED}$, and $\mathcal{C}$ reported in Table III of Supplemental Material [53], at N3LO we find

$$\delta r^2|_e = 1.0758(15)\ \text{fm}^2. \tag{13}$$

We only find a weak modification of the central value compared to the result in Ref. [24] $\delta r^2|_e = 1.0757(15)$, which used Refs. [40,63]. This highlights the weak sensitivity of ordinary helium atoms to nuclear polarizabilities.

In Fig. 3, we present our values of δr^2 (red) at N3LO in comparison to previous extractions by Schumann *et al.* [21] and van der Werf *et al.* [24], along with other experimental results, also shown in Fig. 5 of Ref. [21]. While the van der Werf *et al.* datum remains mostly unchanged due to the insignificance of nuclear structure corrections in ordinary atoms, our updated analysis moves the muonic atom datum the left, enhancing the discrepancy to a 4σ level.

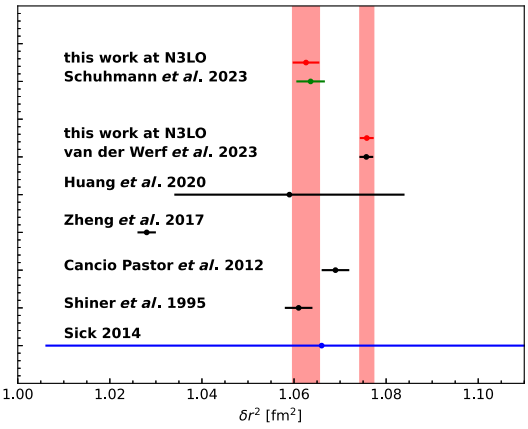

FIG. 3. Our δr^2 results at N3LO (red) compared to the muonic helium extraction by Schumann *et al.* [21] (green) and the ordinary atom extraction (black) by van der Werf *et al.* [24]. Shown are also previous ordinary atom extractions (black) by Shiner *et al.* [25], Cancio Pastor *et al.* [26], Zheng *et al.* [27], Huang *et al.* [28], and the electron scattering data (blue) by Sick [64].

Conclusions—We have calculated nuclear structure corrections in muonic and ordinary helium atoms using accurate few-body methods and χEFT interactions at various orders. With respect to muonic atoms, while various chiral orders were previously explored for muonic deuterium [65,66], this is accomplished here for three- and four-body nuclei. Ordinary helium atoms are analyzed here from a consistent theoretical point of view for the first time.

We applied Bayesian inference techniques to quantify uncertainties stemming from the χEFT truncation. For muonic atoms, this allows us to improve previous simple estimates [34] based on comparing the N3LO chiral and the AV18 + UIX phenomenological interactions. At N3LO, the obtained Bayesian uncertainty is comparable to the previous ones, but is now founded on solid statistical ground. To bring the muonic-atom extraction of δr^2 in agreement with that from ordinary atoms, $\delta\mu$ would have to change by 0.00875 fm^2. This change is excluded by our Bayesian analysis at the 95% confidence level. Conversely, to bring ordinary atom measurements in agreement with the results from muonic atoms, δe would have to be 8 times larger as well as the opposite sign. This is excluded by our Bayesian analysis, as well as from the evidence that ^{4}He is more strongly bound than ^{3}He, and therefore a change of sign is not expected.

Overall, the helium isotope-shift puzzle (see Fig. 3) is not resolved, but rather enhanced to a 4σ level. Therefore, our theoretical analysis suggests that most likely the explanation of the puzzle is related to underestimated systematic errors in the experiment or neglected correction terms.

Acknowledgments—We acknowledge useful discussions with N. Barnea, D. Phillips, R. Pohl, and K. Pachucki. This work was supported by the Deutsche Forschungsgemeinschaft (DFG) through the Cluster of Excellence "Precision Physics, Fundamental Interactions, and Structure of Matter" (PRISMA$^+$ EXC 2118/1) funded by the DFG within the German Excellence Strategy (Project ID No. 390831469).

[1] J. J. Sakurai and Jim Napolitano, *Modern Quantum Mechanics*, 2nd ed. (Cambridge University Press, Cambridge, England, 2017), 10.1017/9781108587280.
[2] David J. Griffiths and Darrell F. Schroeter, *Introduction to Quantum Mechanics*, 3rd ed. (Cambridge University Press, Cambridge, England, 2018), 10.1017/9781316995433.
[3] Paul A. M. Dirac, The quantum theory of the electron, Proc. R. Soc. A **117**, 610 (1928).
[4] Willis E. Lamb and Robert C. Retherford, Fine structure of the hydrogen atom by a microwave method, Phys. Rev. **72**, 241 (1947).

[5] Sin-Itiro Tomonaga and J. R. Oppenheimer, On infinite field reactions in quantum field theory, Phys. Rev. **74**, 224 (1948).

[6] Julian Schwinger, On quantum-electrodynamics and the magnetic moment of the electron, Phys. Rev. **73**, 416 (1948).

[7] R. P. Feynman, Space-time approach to quantum electrodynamics, Phys. Rev. **76**, 769 (1949).

[8] Axel Beyer *et al.*, The Rydberg constant and proton size from atomic hydrogen, Science **358**, 79 (2017).

[9] Hélène Fleurbaey, S. Galtier, S. Thomas, M. Bonnaud, L. Julien, F. Biraben, F. Nez, M. Abgrall, and J. Guena, New measurement of the $1s - 3s$ transition frequency of hydrogen: Contribution to the proton charge radius puzzle, Phys. Rev. Lett. **120**, 183001 (2018).

[10] N. Bezginov, T. Valdez, M. Horbatsch, A. Marsman, A. C. Vutha, and E. A. Hessels, A measurement of the atomic hydrogen Lamb shift and the proton charge radius, Science **365**, 1007 (2019).

[11] Julian J. Krauth, Laura S. Dreissen, Charlaine Roth, Elmer L. Gründeman, Mathieu Collombon, Maxime Favier, and Kjeld S. E. Eikema, Paving the way for fundamental physics tests with singly-ionized helium, Proc. Sci. FFK2019 (**2019**) 049.

[12] Krzysztof Pachucki, Vojtěch Patkóš, and Vladimir A. Yerokhin, Testing fundamental interactions on the helium atom, Phys. Rev. A **95**, 062510 (2017).

[13] Vojtěch Patkóš, Vladimir A. Yerokhin, and Krzysztof Pachucki, Complete $\alpha^7 m$ Lamb shift of helium triplet states, Phys. Rev. A **103**, 042809 (2021).

[14] Eite Tiesinga, Peter J. Mohr, David B. Newell, and Barry N. Taylor, Codata recommended values of the fundamental physical constants: 2018, Rev. Mod. Phys. **93**, 025010 (2021).

[15] Aldo Antognini, Franziska Hagelstein, and Vladimir Pascalutsa, The proton structure in and out of muonic hydrogen, Annu. Rev. Nucl. Part. Sci. **72**, 389 (2022).

[16] Aldo Antognini *et al.*, Muonic-atom spectroscopy and impact on nuclear structure and precision QED theory, arXiv:2210.16929.

[17] Randolf Pohl *et al.*, The size of the proton, Nature (London) **466**, 213 (2010).

[18] Aldo Antognini *et al.*, Proton structure from the measurement of 2s-2p transition frequencies of muonic hydrogen, Science **339**, 417 (2013).

[19] Randolf Pohl *et al.*, Laser spectroscopy of muonic deuterium, Science **353**, 669 (2016).

[20] J. J. Krauth *et al.*, Measuring the α-particle charge radius with muonic helium-4 ions, Nature (London) **589**, 527 (2021).

[21] Karsten Schuhmann *et al.*, The helion charge radius from laser spectroscopy of muonic helium-3 ions, arXiv:2305.11679.

[22] R. van Rooij, J. S. Borbely, J. Simonet, M. D. Hoogerland, K. S. E. Eikema, R. A. Rozendaal, and W. Vassen, Frequency metrology in quantum degenerate helium: Direct measurement of the $2\,^3s_1 \rightarrow 2\,^1s_0$ transition, Science **333**, 196 (2011).

[23] R. J. Rengelink, Y. van der Werf, R. P. M. J. W. Notermans, R. Jannin, K. S. E. Eikema, M. D. Hoogerland, and W. Vassen, Precision spectroscopy of helium in a magic wavelength optical dipole trap, Nat. Phys. **14**, 1132 (2018).

[24] Y. van der Werf, K. Steinebach, R. Jannin, H. L. Bethlem, and K. S. E. Eikema, The alpha and helion particle charge radius difference from spectroscopy of quantum-degenerate helium, arXiv:2306.02333.

[25] D. Shiner, R. Dixson, and V. Vedantham, Three-nucleon charge radius: A precise laser determination using ^{3}He, Phys. Rev. Lett. **74**, 3553 (1995).

[26] P. Cancio Pastor, L. Consolino, G. Giusfredi, P. De Natale, M. Inguscio, V. A. Yerokhin, and K. Pachucki, Frequency metrology of helium around 1083 nm and determination of the nuclear charge radius, Phys. Rev. Lett. **108**, 143001 (2012).

[27] X. Zheng, Y. R. Sun, J.-J. Chen, W. Jiang, K. Pachucki, and S.-M. Hu, Measurement of the frequency of the $2^3s - 2^3p$ transition of ^{4}He, Phys. Rev. Lett. **119**, 263002 (2017).

[28] Yi-Jan Huang, Yu-Chan Guan, Jin-Long Peng, Jow-Tsong Shy, and Li-Bang Wang, Precision laser spectroscopy of the $2^1s_0 - -3^1d_2$ two-photon transition in ^{3}He, Phys. Rev. A **101**, 062507 (2020).

[29] J. L. Friar, Nuclear polarization corrections to μ-d atoms in zero-range approximation, Phys. Rev. C **88**, 034003 (2013).

[30] Krzysztof Pachucki, Vadim Lensky, Franziska Hagelstein, Simone Salvatore Li Muli, Sonia Bacca, and Randolf Pohl, Comprehensive theory of the Lamb shift in light muonic atoms, Rev. Mod. Phys. **96**, 015001 (2024).

[31] Marc Diepold, Beatrice Franke, Julian J. Krauth, Aldo Antognini, Franz Kottmann, and Randolf Pohl, Theory of the Lamb shift and fine structure in muonic ^4He ions and the muonic $^3He - ^4He$ isotope shift, Ann. Phys. (Amsterdam) **396**, 220 (2018).

[32] Beatrice Franke, Julian J. Krauth, Aldo Antognini, Marc Diepold, Franz Kottmann, and Randolf Pohl, Theory of the $n = 2$ levels in muonic helium-3 ions, Eur. Phys. J. D **71**, 341 (2017).

[33] C. Ji, N. Nevo Dinur, S. Bacca, and N. Barnea, Nuclear polarization corrections to the μ^4He$^+$ Lamb shift, Phys. Rev. Lett. **111**, 143402 (2013).

[34] C Ji, S Bacca, N Barnea, O J Hernandez, and N Nevo Dinur, *Ab initio* calculation of nuclear-structure corrections in muonic atoms, J. Phys. G **45**, 093002 (2018).

[35] J. L. Friar and G. L. Payne, Higher-order nuclear-size corrections in atomic hydrogen, Phys. Rev. A **56**, 5173 (1997).

[36] Krzysztof Pachucki, Nuclear structure corrections in muonic deuterium, Phys. Rev. Lett. **106**, 193007 (2011).

[37] Krzysztof Pachucki and Albert Wienczek, Nuclear structure effects in light muonic atoms, Phys. Rev. A **91**, 040503(R) (2015).

[38] Simone Salvatore Li Muli, Bijaya Acharya, Oscar Javier Hernandez, and Sonia Bacca, Bayesian analysis of nuclear polarizability corrections to the Lamb shift of muonic H-atoms and He-ions, J. Phys. G **49**, 105101 (2022).

[39] J. L. Friar and G. L. Payne, Higher-order nuclear-polarizability corrections in atomic hydrogen, Phys. Rev. C **56**, 619 (1997).

[40] K. Pachucki and A. M. Moro, Nuclear polarizability of helium isotopes in atomic transitions, Phys. Rev. A **75**, 032521 (2007).

[41] Nir Barnea, Winfried Leidemann, and Giuseppina Orlandini, State dependent effective interaction for the hyperspherical formalism, Phys. Rev. C **61**, 054001 (2000).
[42] H. Kamada *et al.*, Benchmark test calculation of a four-nucleon bound state, Phys. Rev. C **64**, 044001 (2001).
[43] N. Nevo Dinur, N. Barnea, C. Ji, and S. Bacca, Efficient method for evaluating energy-dependent sum rules, Phys. Rev. C **89**, 064317 (2014).
[44] Simone Salvatore Li Muli, Sonia Bacca, and Nir Barnea, Implementation of local chiral interactions in the hyperspherical harmonics formalism, Front. Phys. **9** (2021).
[45] S. Weinberg, Effective chiral Lagrangians for nucleon-pion interactions and nuclear forces, Nucl. Phys. **B363**, 3 (1991).
[46] S. Weinberg, Three-body interactions among nucleons and pions, Phys. Lett. B **295**, 114 (1992).
[47] R. Machleidt and D. R. Entem, Chiral effective field theory and nuclear forces, Phys. Rep. **503**, 1 (2011).
[48] Evgeny Epelbaum, Hermann Krebs, and Patrick Reinert, Semi-local nuclear forces from chiral EFT: State-of-the-art and challenges, in *Handbook of Nuclear Physics*, edited by Isao Tanihata, Hiroshi Toki, and Toshitaka Kajino (Springer, Singapore, 2022), pp. 1–25, 10.1007/978-981-15-8818-1_54-1.
[49] Bijaya Acharya, S. Bacca, F. Bonaiti, S. S. Li Muli , and Joanna E. Sobczyk, Uncertainty quantification in electromagnetic observables on nuclei, Front. Phys. **10** (2023).
[50] A. Gezerlis, I. Tews, E. Epelbaum, M. Freunek, S. Gandolfi, K. Hebeler, A. Nogga, and A. Schwenk, Local chiral effective field theory interactions and quantum Monte Carlo applications, Phys. Rev. C **90**, 054323 (2014).
[51] J. Lynn, I. Tews, J. Carlson, S. Gandolfi, A. Gezerlis, K. E. Schmidt, and A. Schwenk, Chiral three-nucleon interactions in light nuclei, neutron-α scattering and neutron matter, Phys. Rev. Lett. **116**, 062501 (2016).
[52] J. E. Lynn, I. Tews, J. Carlson, S. Gandolfi, A. Gezerlis, K. E. Schmidt, and A. Schwenk, Quantum Monte Carlo calculations of light nuclei with local chiral two- and three-nucleon interactions, Phys. Rev. C **96**, 054007 (2017).
[53] See Supplemental Material at http://link.aps.org/supplemental/10.1103/PhysRevLett.134.032502 for uncertainty quantification details.
[54] D. R. Entem and R. Machleidt, Accurate charge-dependent nucleon-nucleon potential at fourth order of chiral perturbation theory, Phys. Rev. C **68**, 041001(R) (2003).
[55] P. Navrátil, Local three-nucleon interaction from chiral effective field theory, Few-Body Syst. **41**, 117 (2007).
[56] N. Nevo Dinur, C. Ji, S. Bacca, and N. Barnea, Nuclear structure corrections to the Lamb shift in μhe + 3 and μh3, Phys. Lett. B **755**, 380 (2016).
[57] A. Gnech, L. E. Marcucci, and M. Viviani, Bayesian analysis of muon capture on the deuteron in chiral effective field theory, Phys. Rev. C **109**, 035502 (2024).
[58] J. E. Sobczyk, S. Bacca, G. Hagen, and T. Papenbrock, Spectral function for ^{4}He using the Chebyshev expansion in coupled-cluster theory, Phys. Rev. C **106**, 034310 (2022).
[59] H. Jeffreys, *Theory of Probability* (Oxford University Press, 1939), 10.1093/oso/9780198503682.001.0001.
[60] S. Wesolowski, R. J. Furnstahl, J. A. Melendez, and D. R. Phillips, Exploring Bayesian parameter estimation for chiral effective field theory using nucleon–nucleon phase shifts, J. Phys. G **46**, 045102 (2019).
[61] R. J. Furnstahl, N. Klco, D. R. Phillips, and S. Wesolowski, Quantifying truncation errors in effective field theory, Phys. Rev. C **92**, 024005 (2015).
[62] Krzysztof Pachucki and V. A. Yerokhin, Theory of the helium isotope shift, J. Phys. Chem. Ref. Data **44**, 031206 (2015).
[63] Vojtěch Patkóš, Vladimir A. Yerokhin, and Krzysztof Pachucki, Higher-order recoil corrections for singlet states of the helium atom, Phys. Rev. A **95**, 012508 (2017).
[64] Ingo Sick, Zemach moments of ^{3}He and ^{4}He, Phys. Rev. C **90**, 064002 (2014).
[65] O. J. Hernandez, C. Ji, S. Bacca, N. Nevo Dinur, and N. Barnea, Improved estimates of the nuclear structure corrections in μd, Phys. Lett. B **736**, 344 (2014).
[66] O. J. Hernandez, A. Ekström, N. Nevo Dinur, C. Ji, S. Bacca, and N. Barnea, The deuteron-radius puzzle is alive: A new analysis of nuclear structure uncertainties, Phys. Lett. B **778**, 377 (2018).